A molecular dynamics study of the diffusion processes in liquid Na-K alloys

A molecular dynamics study of the diffusion processes in liquid Na–K alloys

A Baumketner† and Ya Chushak

Institute for Condensed Matter Physics, 1 Svientsitskogo Street, Lviv 290011, Ukraine

Abstract. Molecular dynamics simulations are used to investigate the diffusion processes in the liquid metal alloys Na_cK_{1-c} at three different concentrations. Self-correlation and distinct velocity correlation functions together with the corresponding diffusion coefficients have been calculated and analysed in order to study the phase-separation phenomenon. It is found that Na_3K_7 and Na_5K_5 compositions display significant dynamic cross correlations indicating a demixing behaviour for these alloys, whereas Na_8K_2 alloy is a nearly ideal mixture. The results obtained agree well with the experimental observation of a tendency towards phase separation exhibited by liquid Na–K alloys.

1. Introduction

During the last few years, remarkable progress has been made in the theoretical description of the diffusion processes in binary liquids [1–6]. The main quantities of interest are self- and mutual diffusion coefficients. The two self-diffusion coefficients D_i ($i = 1, 2$) are related to the motion of a tagged, isolated particle of species i through a uniform medium, whereas the mutual (or interdiffusion) coefficient D_m describes the collective transport of mass driven by gradients in chemical potentials. Molecular dynamics simulation plays an essential role in the study of diffusion properties of liquids, since it allows the motion of each particle to be 'observed' on atomic scales of length and time [7]. The self- and mutual diffusion coefficients may be calculated as the Green–Kubo integrals of the self- and distinct velocity correlation functions (VCFs) or from the corresponding mean square displacements, directly accessible in MD simulations. The dynamical cross correlation ratio defined as $\delta D = D_m/D_m^0$, where D_m^0 is the mutual diffusion coefficient of an ideal mixture, is well suited to the study of the phase-separation or inverse phenomena in binary liquids. For values $\delta D > 1$, phase-separation trends are displayed by the mixture, while $\delta D < 1$ indicates an associative behaviour [1].

   However, the recent theoretical study of the diffusion processes in binary liquids has mainly been focused on molten salts and various modifications of Lennard-Jones systems [1–5, 9, 10]. The aim of this paper is to analyse the VCFs and related diffusion coefficients in liquid metal alloys Na–K at different concentrations. Recently, the static structure of liquid Na–K alloys, interacting via effective pair potentials derived from the neutral-pseudoatom method, has been studied by means of the integral-equation theory [8]. The calculated static structure factors predict a phase-separating character for this alloy, in good agreement with experimental data.

† Author to whom any correspondence should be addressed. E-mail address: `andrij@icmp.lviv.ua`.

In the present calculations we use the same pair potentials for MD simulations of sodium–potassium alloys at three different concentrations: Na_3K_7, Na_5K_5 and Na_8K_2, and analyse the dynamic cross correlations in these alloys with respect to the phase-separation phenomenon.

2. Basic theory

2.1. Self- and distinct diffusion coefficients

The dynamic functions in which we are mainly interested are: two velocity autocorrelation functions of each species:

$$Z_i(t) = \frac{1}{3N_i} \sum_j \langle \vec{v}_j^i(t) \cdot \vec{v}_j^i(0) \rangle \tag{1}$$

and the time correlation function (TCF) of the velocity of the centre of mass of the first component:

$$Z_{cm}(t) = \frac{N}{3} \langle \vec{u}^1(t) \cdot \vec{u}^1(0) \rangle \qquad \vec{u}^1(t) = \frac{1}{N_1} \sum_j \vec{v}_j^1(t). \tag{2}$$

Here, $\vec{v}_j^i(t)$ is the velocity of the jth particle of species i at time t, N_i is the number of particles of species i and $N = N_1 + N_2$ is the total number of particles. The angular brackets $\langle \cdots \rangle$ denote the time average. The diffusion coefficients (DCs) are given by the Green–Kubo integrals of the corresponding VCFs:

$$D_i = \int_0^\infty Z_i(t) \, dt \tag{3}$$

and

$$D_m = \frac{(c_1 c_2)^2}{S_{cc}(0)} \left(1 + \frac{m_1 c_1}{m_2 c_2}\right)^2 \int_0^\infty Z_{cm}(t) \, dt \tag{4}$$

where c_i, m_i represent the concentration and mass of particles of the ith component, and $S_{cc}(0)$ is the long-wavelength limit of the Bhatia–Thornton concentration–concentration structure factor.

The mutual (or distinct) diffusion coefficient is related to its self-counterparts via [4]

$$D_m = \frac{c_1 c_2}{S_{cc}(0)} \left(c_1 D_2 + c_2 D_1 + c_1 c_2 \int_0^\infty \left[\Lambda_{11}^d(t) + \Lambda_{22}^d(t) - 2\Lambda_{12}^d(t) \right] \, dt \right) \tag{5}$$

where $\Lambda_{ij}^d(t)$ are distinct or cross velocity correlation functions:

$$\Lambda_{ij}^d(t) = \frac{1}{3} N \langle \vec{v}_k^i(t) \cdot \vec{v}_l^j(0) \rangle \qquad (k \neq l \text{ if } i = j). \tag{6}$$

In the ideal mixture, the dynamic cross correlations are absent and

$$D_m^0 = \frac{c_1 c_2}{S_{cc}(0)} (c_2 D_1 + c_1 D_2). \tag{7}$$

It is well known that the distinct velocity correlation functions and related D_m, unlike the self-diffusion properties, depend on a reference system. Raineri and Friedman showed [6] that the constant-energy (NVE) MD ensemble is equivalent to the fixed-mass or barycentric reference frame (RF). Hence, using relationships between VCFs that hold in this RF, we can

express the Λ functions in terms of the introduced Z-functions as follows:

$$\Lambda_{11}^d(t) = Z_{cm}(t) - \frac{Z_1(t)}{c_1}$$

$$\Lambda_{22}^d(t) = \left(\frac{c_1 m_1}{c_2 m_2}\right)^2 Z_{cm}(t) - \frac{Z_2(t)}{c_2} \tag{8}$$

$$\Lambda_{12}^d(t) = -\frac{c_1 m_1}{c_2 m_2} Z_{cm}(t)$$

with the initial values

$$Z_i(0) = \frac{k_B T}{m_i} \qquad Z_{cm}(0) = \frac{k_B T}{\bar{m}} \frac{m_2 c_2}{m_1 c_1} \tag{9}$$

$$\Lambda_{11}^d(0) = \Lambda_{22}^d(0) = \Lambda_{12}^d(0) = -\frac{k_B T}{\bar{m}} \tag{10}$$

where $\bar{m}$ is the mean mass: $\bar{m} = c_1 m_1 + c_2 m_2$.

The sum function $\Lambda^s(t) = \Lambda_{11}^d(t) + \Lambda_{22}^d(t) - 2\Lambda_{12}^d(t)$ characterizes dynamical cross correlations in binary liquids. The time integral over the sum function $I^s = \int \Lambda^s(t) \, dt$ is zero for a dynamically ideal mixture and $I^s > 0$ for mixtures with a tendency towards phase separation. Quantitatively, the system's deviation from ideality is measured by the cross correlation ratio δD.

The Green–Kubo formulae for the DCs are evaluated by integrating the corresponding correlation functions over the time interval from zero to infinity. In practice, however, the upper limit of integration is rarely greater than a few picoseconds. Alternatively, diffusion coefficients may be calculated from the corresponding mean square displacement (MSD)

$$\langle r^2(t) \rangle_i = \langle [\vec{r}^i(t) - \vec{r}^i(0)]^2 \rangle \tag{11}$$

$$\langle R^2(t) \rangle_1 = \langle [\vec{R}_1(t) - \vec{R}_1(0)]^2 \rangle \tag{12}$$

using the Einstein relations [13]

$$D_i = \frac{1}{6} \lim_{t \to \infty} \frac{\langle r^2(t) \rangle_i}{t} \tag{13}$$

and

$$D_m = \frac{N}{6} \frac{(c_1 c_2)^2}{S_{cc}(0)} \left(1 + \frac{m_1 c_1}{m_2 c_2}\right)^2 \lim_{t \to \infty} \frac{\langle R^2(t) \rangle_1}{t} \tag{14}$$

where $\vec{r}^i(t)$ is the position of an arbitrary particle of species i and $\vec{R}_1(t)$ is the position of the centre of mass of component 1 at time t.

The third method suitable for the evaluation of DCs is through the incoherent

$$F_i^s(q, t) = \frac{1}{N_i} \sum_j^{N_i} \langle \exp[-i\vec{q} \cdot (\vec{r}_j^i(t) - \vec{r}_j^i(0))] \rangle \tag{15}$$

and concentration–concentration

$$F_{cc}(q, t) = N \langle c_q(t) c_{-q}(0) \rangle \tag{16}$$

intermediate-scattering functions, where

$$c_q(t) = \frac{1}{N} \left(c_2 \sum_j^{N_1} \exp(-i\vec{q} \cdot \vec{r}_j^1(t)) - c_1 \sum_j^{N_2} \exp(-i\vec{q} \cdot \vec{r}_j^2(0)) \right). \tag{17}$$

The hydrodynamic form of $F_i^s(q, t)$ is related to the self-diffusion coefficient D_i [13] by

$$F_i^s(q, t) = \exp(-D_i q^2 t). \tag{18}$$

The second function, $F_{cc}(q, t)$, is connected with the mutual diffusion constant in the hydro-dynamic limit by

$$F_{cc}(q, t) = (S_{cc}(q)/A) \left[\left(D_m - \frac{D_T + \mathcal{D} - A}{2} \right) \exp \left\{ -\frac{q^2}{2} t[(D_T + \mathcal{D}) + A] \right\} \right.$$
$$\left. - \left(D_m - \frac{D_T + \mathcal{D} + A}{2} \right) \exp \left\{ -\frac{q^2}{2} t[(D_T + \mathcal{D}) - A] \right\} \right] \tag{19}$$

where $A = \sqrt{(D_T + \mathcal{D})^2 - 4 D_T D_m}$, D_T is the thermal diffusion coefficient, $\mathcal{D} = D_m(1 + \alpha)$ and α is a combination of some thermodynamic quantities that we are not actually interested in. Note that because as many as three fitting parameters are involved in this formula, the results obtained are not very precise and must be regarded with a good deal of scepticism. Nevertheless expression (19) can serve as an indirect check of $S_{cc}(0)$ since it gives D_m itself whereas equations (14) and (4) give only the product $S_{cc}(0) D_m$. The fitting procedures were carried out over the time range $t > t_c$ where t_c indicates the beginning of the linear time dependency of the mean square displacement.

It should also be noted that equations (18) and (19) assume that the wavevector q is small enough for probing the hydrodynamic limit. If this is not so, we can only speak of the q-dependent generalized $D_i(q)$ and $D_m(q)$. Finally, we would like to list all TCFs that were directly calculated during the MD runs: $\langle r^2(t) \rangle_i$, $\langle R^2(t) \rangle_1$, $Z_i(t)$, $Z_{cm}(t)$, $F_i^s(q, t)$ and $F_{cc}(q, t)$.

2.2. Calculation of $S_{cc}(0)$

If we are interested in the absolute value of the mutual diffusion coefficient D_m, an evaluation of $S_{cc}(0)$ is inevitable. Unfortunately, the fixed number of particles in MD simulations [11] produces a significant error in the estimation of the structure factor in the low-q region. Therefore, we have applied a finite-size correction procedure to the pair distribution functions (PDFs) obtained in MD simulations [14]. Our approach is based on the Taylor-series expansion of the pair distribution function for the infinite system $g_{ij}(r)$ about an average number of particles to order $1/N$:

$$g_{ij}(r) = g_{ij}^N(r) + \sum_{\alpha\beta=1,2} \frac{\sqrt{N_\alpha N_\beta} S_{\alpha\beta}(0)}{2 N_i N_j} \frac{\partial}{\partial \rho_\alpha} \frac{\partial}{\partial \rho_\beta} \left[\rho_i \rho_j g_{ij}(r) \right] \tag{20}$$

where $g_{ij}^N(r)$ is the PDF for an N-particle system, obtained in a MD simulation, ρ_i is the number density of particles of the ith sort and $S_{ij}(0)$ is the Ashcroft–Langreth static structure factor. In this expression we replace the $g_{ij}(r)$ under derivation in the right-hand side with the PDFs calculated by means of the integral-equation technique in the modified hypernetted-chain (MHNC) approximation with bridge functions derived in the *Mori–Hoshino–Watabe* (MHW) scheme [12]. This method contains no adjustable parameters and is thought to generate PDFs in good agreement with MD data for liquid metal alloys.

The finite-size correction procedure is arranged into a sequence of steps. In the first step we use the $S_{ij}(0)$ predicted by the MHNC theory to make the correction to the MD PDFs $g_{ij}^N(r)$ via expression (20). This may be done only in the limited separation range $r < L/2$, where L is the length of the simulation box. To evaluate PDFs beyond that range, we used a procedure proposed by Galam and Hansen [15] which consists in solving the Ornstein–Zernike (O–Z) equation with the following closure:

$$c_{ij}(r) = \begin{cases} g_{ij}(r) - 1 - \gamma_{ij}(r) & \text{if } r < R_{ij}^c \\ -\beta U_{ij}^c(r) & \text{if } r > R_{ij}^c. \end{cases} \tag{21}$$

Here, $c_{ij}(r)$ is the direct correlation function, $\gamma_{ij}(r) = g_{ij}(r) - 1 - c_{ij}(r)$ and $U_{ij}^c(r)$ is the cut effective potential used in the simulation. The cut-off radius R_{ij}^c should be chosen from the third to the fourth potential minimum for the best result [16]. Now, the PDFs obtained over the full range of r may be safely Fourier transformed to determine new values of $S_{ij}(0)$ and to return to the correction step. This loop is repeated until self-consistency between the initial and final $S_{ij}(0)$ is achieved. In practice it takes no more than four or five iterations.

Up to this point we have constructed the structure functions for a system interacting not via actual potentials $U_{ij}(r)$ but via the cut potentials used in the MD simulation. To determine $S_{ij}(0)$ for the system with full potentials, we must exploit the fact that the bridge functions $B_{ij}(r)$ are less sensitive to the long-range tail of the pair potentials than the PDFs are and that the $B_{ij}(r)$ are equal for the two systems [16]. Now, we can derive the bridge functions from the converged $g_{ij}(r)$ via

$$B_{ij}(r) = \gamma_{ij}(r) - \log(\gamma_{ij}(r)) - \beta U_{ij}^c(r) \tag{22}$$

and substitute them into a closure

$$c_{ij}(r) = \exp(-\beta U_{ij}(r) + \gamma_{ij}(r) - B_{ij}(r)) - 1 - \gamma_{ij}(r) \tag{23}$$

and then solve the O–Z equation complemented with it to evaluate the final PDFs and static structure factors.
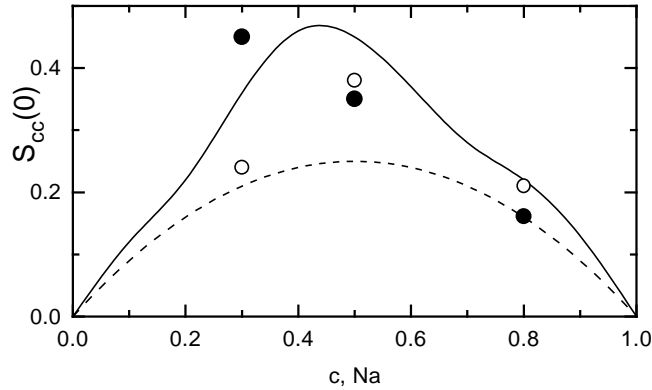
Figure 1. The Bhatia–Thornton structure factor $S_{cc}(0)$ versus concentration. Solid circles: present results; open circles: experimental data given by van der Lugt; full curve: experimental data given by Hultgren *et al*; dotted curve: the ideal-mixture result $S_{cc}(0) = c_1 c_2$.

A system is called thermodynamically ideal when $S_{cc}(0) = c_1 c_2$. If a mixture is preferred to the phase separation, $S_{cc}(0) > c_1 c_2$, and vice versa for an associating mixture. In a real separating system, $S_{cc}(0)$ tends to infinity. Starting from 500- and 2048-particle molecular dynamics ensembles, we managed to calculate $S_{cc}(0)$ differing from each other by no more than 10% for Na_3–K_7 alloy. For the remaining two systems, we expect accuracy that is at least as good. In figure 1 we present the results obtained for $S_{cc}(0)$ as a function of concentration in comparison with the experimental data derived by Hultgren *et al* [17] from the activity experiments and by Alblas and van der Lugt [18] from the x-ray scattering. In general, there is good agreement between theoretical and experimental data, which show a weak tendency towards phase separation for liquid Na–K alloys.
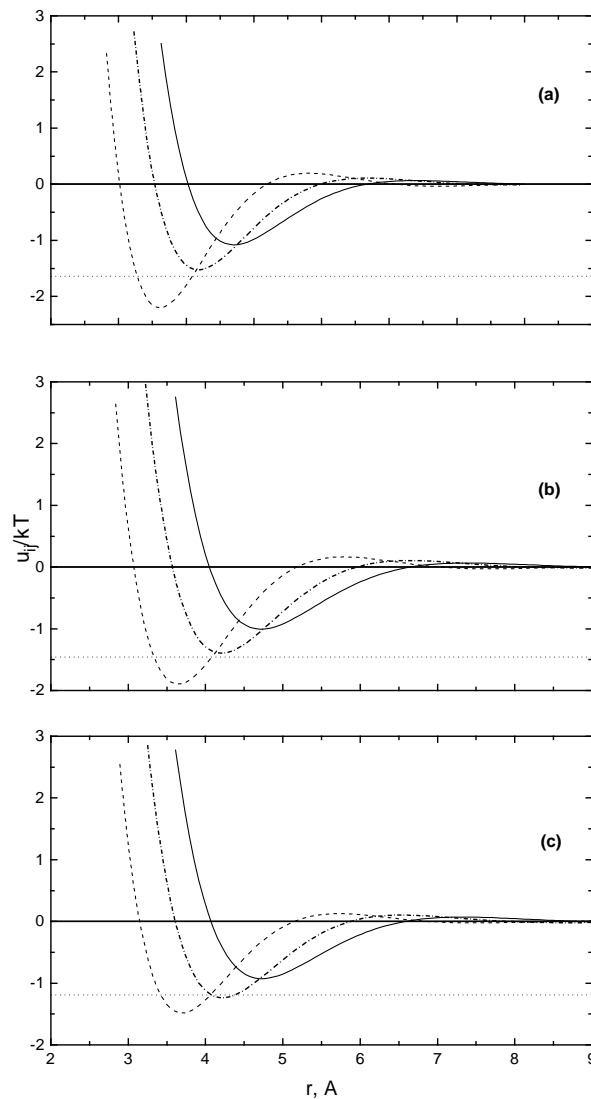
Figure 2. Effective pair potentials $U_{ij}(r)/kT$ for Na–K alloys: from here on, (a) corresponds to Na$_3$K$_7$ alloy, (b) to Na$_5$K$_5$ and (c) to Na$_8$K$_2$. Full curves: K–K; dot–dashed curves: Na–K; dashed curves: Na–Na. The averaged value $\epsilon_{12}^{av} = \frac{1}{2}(\epsilon_{11} + \epsilon_{22})$ is shown by light dotted lines.

3. Results

3.1. Molecular dynamics simulations

We have studied the diffusion properties for three liquid Na–K alloys at a temperature $T = 373$ K: Na$_3$K$_7$ ($\rho = 0.014\,87$ Å^{-3}), Na$_5$K$_5$ ($\rho = 0.016\,83$ Å^{-3}) and Na$_8$K$_2$ ($\rho = 0.020\,68$ Å^{-3}). We used the effective interatomic potentials $U_{ij}(r)$ obtained by Gonzalez *et al* within the neutral-pseudoatom method [8]. Figure 2 shows the interatomic pair potentials for the systems under investigation. It is observed that each of the three sets of potentials is symmetrical with respect to the position of the main minimum of the interaction between unlike

particles, $U_{12}(r)$; thus the cross correlations are primarily governed by the relative magnitude of the interaction strength $\delta\epsilon_{12} = \epsilon_{12}/\epsilon_{12}^{av}$, where $\epsilon_{12}^{av} = \frac{1}{2}(\epsilon_{11} + \epsilon_{22})$ and ϵ_{ij} is the magnitude of the main minimum of $U_{ij}(r)$. The first minimum of $U_{12}(r)$ for Na_3K_7 alloy lies over the averaged value ϵ_{12}^{av} and $\delta\epsilon = 0.93$, which leads to strengthening of the cross correlations and a tendency towards demixing for this composition. As the concentration of Na atoms in the alloy increases, the depth of the first minimum of $U_{12}(r)$ tends to the averaged value and for Na_8K_2 alloy $\delta\epsilon = 1.01$, which leads us to predict a nearly ideal dynamic behaviour for this system.

The simulations have been performed using a micro-canonical ensemble consisting of 500 particles with the usual periodic boundary conditions. The velocity Verlet algorithm was adopted [7] as the best one for such calculations. The time step of about 5×10^{-15} s was sufficient to conserve the total energy of the system to better than 0.01% even for the longest run.

Some remarks are in order concerning the accuracy of the results obtained. Firstly, computation of the one-particle properties (namely $\langle r^2(t) \rangle_1$, $Z_i(t)$ and $F_i^s(q, t)$) is not critical: 400 000 time steps were enough for calculating $Z_i(t)$ with the accuracy of 1%. Collective properties require much longer runs and, for example, to reach the accuracy of 3% for $Z_{cm}(t)$ as many as 1 200 000 time steps were necessary. The second remark is connected with the accuracy of the calculated diffusion coefficients. As mentioned above, we calculated DCs in three different ways. Once the range of linearity of the mean square displacements has been established, it is sufficient to calculate the diffusion coefficients. The Green–Kubo relations, however, require accurate values of the correlation functions over the whole integration time interval. That is why the DCs obtained from the MSD are accurate to up to 1–3% and 4–5% compared with 3–4% and 6–7% of the accuracy from the Green–Kubo relations. We did not estimate the errors for $F_i^s(q, t)$ and $F_{cc}(q, t)$ because they are used in a fitting procedure that produces additional errors. Therefore, the diffusion coefficients from those fits are usually the least precise ones and are mainly used for qualitative comparisons. Finally, we would like to note that we obtain not the mutual diffusion coefficient itself from the Green–Kubo relation or mean square displacement but the product $D_m S_{cc}(0)$, and it is this quantity that is determined with the above-mentioned accuracy. The mutual diffusion coefficient itself is calculated with 15–20% uncertainty due to the additional error in deriving $S_{cc}(0)$.

3.2. Dynamic cross correlations

The distinct correlation functions $\Lambda_{ij}^d(t)$ are moderately interesting in their own right, while the sum function $\Lambda^s(t)$ characterizes the dynamic cross correlations in the system and its time integral I_s directly contributes to the mutual diffusivity. In figure 3 we present $\Lambda_{ij}^d(t)$ along with the sum function $\Lambda^s(t)$ for the three alloys examined in this study. The sum function for all concentrations has oscillatory character with a decreasing importance of the net cross correlations with increasing concentration of the Na component. For Na_3K_7 alloy, $\Lambda^s(t)$ has a large maximum near 0.13 ps resulting from a reduced (compared to the pseudomixture case) momentum exchange between particles of unlike species and leading to a value larger than unity of the dynamic cross correlation ratio δD. For Na_5K_5 alloy, the cross correlation contributions become less pronounced, and eventually almost disappear for Na_8K_2 alloy, indicating hence a nearly ideal behaviour for this composition. This result agrees well with the earlier findings concerning the magnitude of the first minimum of $U_{12}(r)$ and from the concentration–concentration structure factor $S_{cc}(0)$ for these alloys.

Figure 4 shows the spectrum of the normalized velocity correlation functions $Z_i(\omega)$ and $Z_{cm}(\omega)$ in comparison with the function $c_1 Z_2(\omega) + c_2 Z_1(\omega)$, which characterizes the ideal
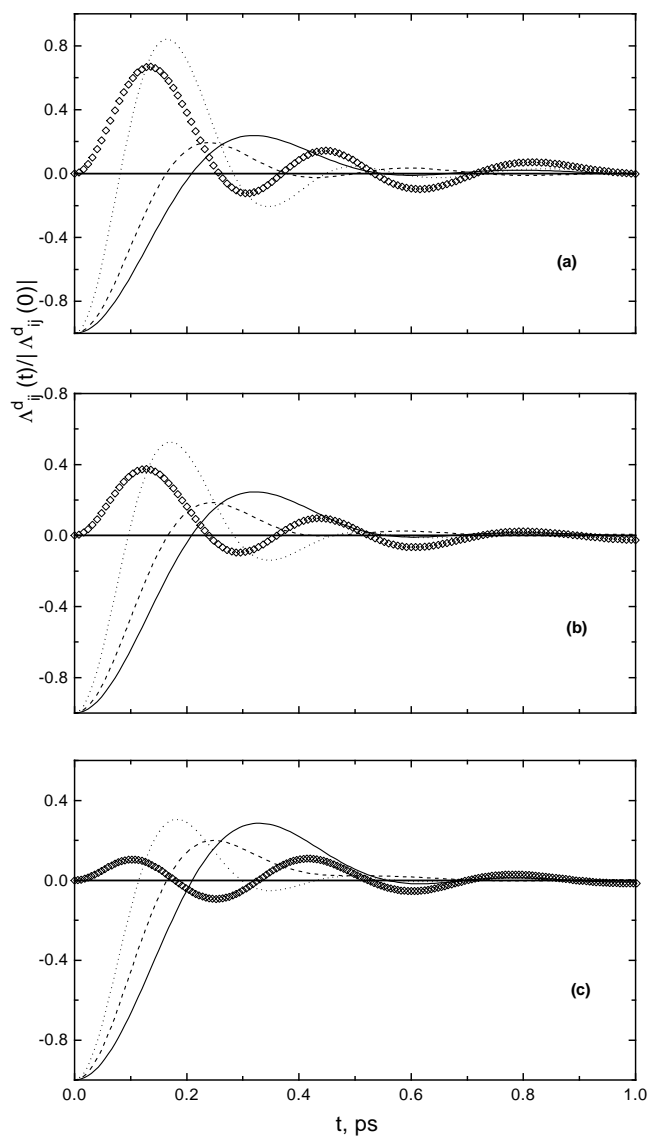
Figure 3. The normalized distinct velocity TCFs $\Lambda^d_{ij}(t)$: full curves: K–K; dashed curves: Na–Na; dotted curves: Na–K; symbols: the sum function $\Lambda^s(t)$.

mixture. These spectra were smoothed by convoluting them with a Gaussian resolution function chosen so as to preserve the zeroth frequency moment. The positions of the maxima of $Z_i(\omega)$ are related to the frequency of oscillations of Na and K atoms in their 'cages' formed by the nearest neighbours, while that of $Z_{cm}(\omega)$ may be interpreted as the main frequency of the oscillations of the components as a whole. It is observed that the oscillations of the light Na atoms give a contribution to the dynamic non-ideality at high frequencies, while the heavier atoms of K do so at lower frequencies. The most relevant dynamic cross correlations occur, however, in the low-ω region of $Z_{cm}(\omega)$. The diffusion coefficients were calculated from these spectra at $\omega = 0$ rather than by direct integration of VCFs, since the statistical
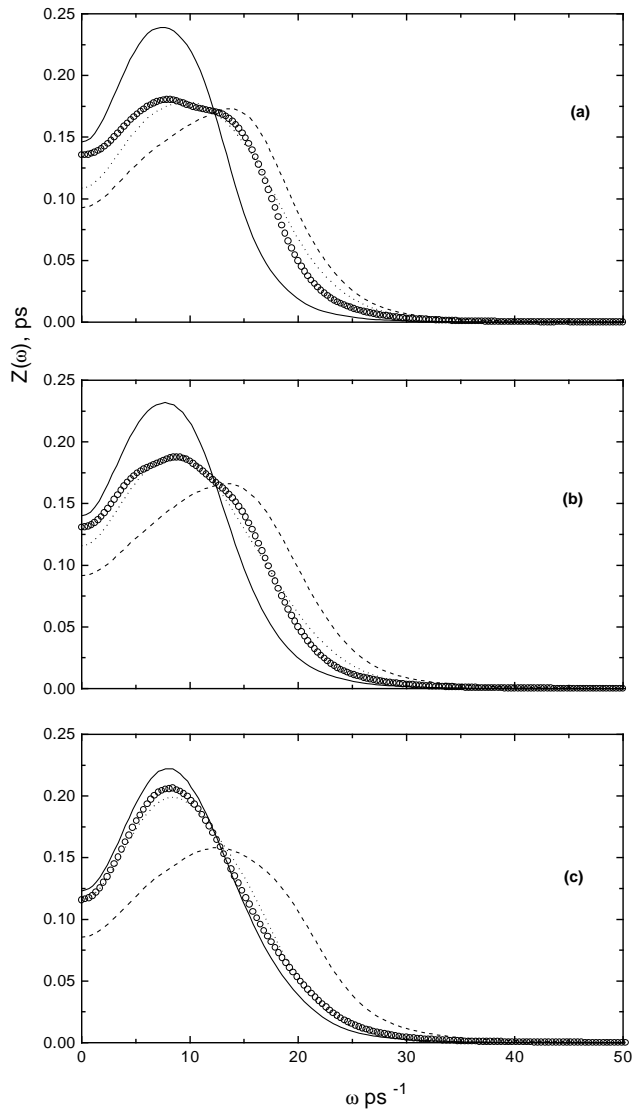
Figure 4. Power spectra of the normalized velocity correlation functions: full curves: $Z^s(\omega)$ for K particles; dashed curves: $Z^s(\omega)$ for Na particles; dotted curves: ideal-mixture results $c_2 Z_1^s(\omega) + c_1 Z_2^s(\omega)$; open circles: centre-of-mass $Z_{cm}(\omega)$.

noise that they contain was substantially reduced by the smoothing procedure. The results for the diffusion coefficients obtained in the three ways described for the alloys studied are compiled in table 1. The self-diffusion coefficients D_i obtained from the fitting of the corresponding incoherent intermediate-scattering function $F_i^s(q, t)$ are in good agreement with the mean square displacement and Green–Kubo results. The mutual diffusion coefficients D_m derived from the fitting of $F_{cc}(q, t)$ are in somewhat poorer agreement due to greater statistical uncertainties of $F_{cc}(q, t)$ and the procedure of fitting.

In figure 5 we present the DCs obtained from the fitting of $F_i^s(q, t)$ and $F_{cc}(q, t)$ at different wavevectors, which may be regarded as the q-dependent generalized diffusion coefficients. It

Table 1. Self- and mutual diffusion coefficients (in $\text{Å}^2 \text{ ps}^{-1}$) for Na–K alloy.

|	Na_3K_7			Na_5K_5			Na_8K_2		
	D_1	D_2	D_m	D_1	D_2	D_m	D_1	D_2	D_m
Green–Kubo	0.58	0.62	0.37	0.56	0.62	0.49	0.49	0.58	0.53
MSD	0.57	0.62	0.36	0.55	0.62	0.49	0.47	0.57	0.54
Fit[a]	0.59	0.65	0.39	0.56	0.63	0.44	0.48	0.58	0.47

[a] The smallest wavevector is $q = 0.19\,\text{Å}^{-1}$ for Na_3K_7; $q = 0.20\,\text{Å}^{-1}$ for Na_5K_5 and $q = 0.22\,\text{Å}^{-1}$ for Na_8K_2 alloy.
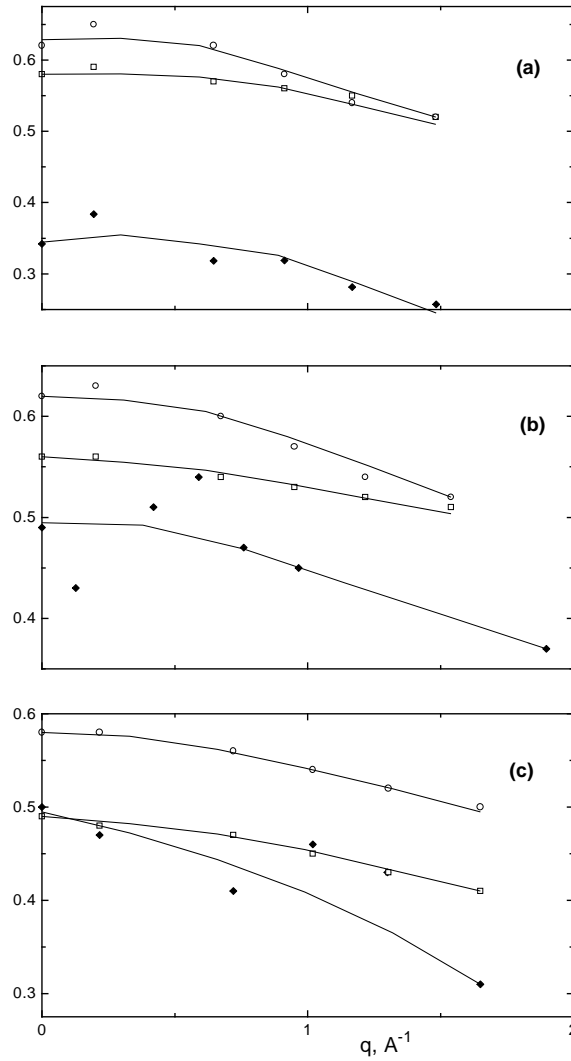
Figure 5. Generalized q-dependent diffusion coefficients for Na–K alloys. Squares: the self-diffusion coefficient $D_2(q)$ for the Na component; circles: the self-diffusion coefficient $D_1(q)$ for K; diamonds: the mutual diffusion coefficient $D_m(q)$.

is found that the self-diffusion coefficients $D_i(q)$ smoothly decrease with q for all three alloys. Such a decreasing behaviour is brought about by deviation of the van Hove self-distribution function $G_s(\vec{r}, t)$ from the Gaussian form, namely by the positive difference between space moments of those functions. This fact may be proven in the kinetic theory approach for dilute gases [19] and has been established for liquids with negligible coupling between self- and collective motions [20].

Calculation of the mutual diffusion constant $D_m(q)$ requires much greater computational effort than that of its self-diffusion counterpart; therefore we did not evaluate $D_m(q)$ at all wavevectors compatible with the size of the MD box. But even for those values of q for which the calculations were performed, the error in $D_m(q)$ is so large that we failed to resolve any fine structure with q.
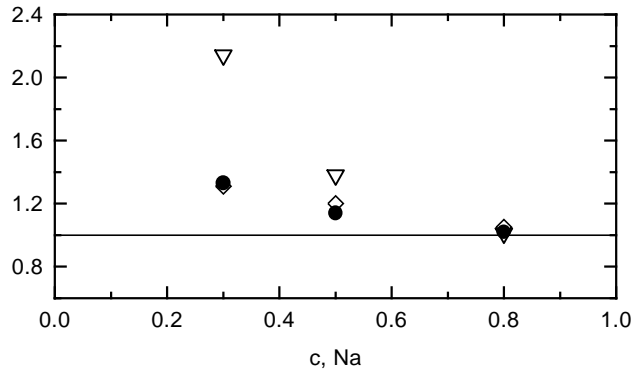
Figure 6. Cross correlations in Na–K alloy as a function of concentration. Symbols: solid circles: dynamic cross correlations D_m/D_m^0; diamonds: static cross correlations $(g_{11}+g_{22})/2g_{12}$; triangles: 'thermodynamic' cross correlations $S_{cc}(0)/c_1 c_2$.

The dynamic cross correlation ratio $\delta D = D_m/D_m^0$ for Na–K alloys as a function of composition is presented in figure 6. As mentioned, δD for all systems studied is larger than unity, thus revealing the tendency towards segregation exhibited by the alloy. For comparison, we also depicted the static cross correlations defined as [1] $(g_{11} + g_{22})/2g_{12}$ where g_{ij} is the magnitude of the first maximum of the corresponding pair correlation function $g_{ij}(r)$. The static and dynamic cross correlations show very similar weak concentration dependence. In contrast, the 'thermodynamic' ratio of $S_{cc}(0)$ to its ideal value, $S_{cc}(0)/c_1 c_2$, depends rather strongly on the alloy composition. However, all criteria—the static, dynamic and thermodynamic— indicate the ideal-mixture behaviour for $Na_8 K_2$ alloy and predict a tendency towards phase separation for $Na_5 K_5$ and $Na_3 K_7$ compositions.

4. Conclusions

We have presented a molecular dynamics simulation study of the diffusion processes in liquid metal alloys Na–K exhibiting a tendency towards phase separation. The self- and mutual diffusion coefficients were calculated in three different ways: by using the Einstein relation derived from the mean square displacements, by using the Green–Kubo relation for the velocity correlation functions and by fitting the incoherent or concentration–concentration intermediate-scattering functions. We also calculated the distinct velocity correlation function which characterizes the dynamic cross correlations in the system. A special effort has been

made to obtain the correct value of $S_{cc}(0)$. To this end, we applied the finite-size correction to the pair distribution functions obtained in MD simulations and extended them into the large-r region by means of the integral-equation technique.

The analysis of the dynamic cross correlations in the liquid Na–K system clearly showed the existence of a tendency towards phase separation for Na_3K_7 and Na_5K_5 alloys, while Na_8K_2 alloy exhibits a nearly ideal behaviour. This result agrees well with the experimental findings for the long-wavelength limit of the concentration–concentration structure factor $S_{cc}(0)$ for these alloys.

Acknowledgments

References

[1] Schoen M and Hoheisel C 1984 *Mol. Phys.* **52** 1029
     Schoen M and Hoheisel C 1984 *Mol. Phys.* **53** 1367
[2] Vogelsang R, Hoheisel C, Paolini G V and Ciccotti G 1987 *Phys. Rev.* A **36** 3964
[3] Vogelsang R and Hoheisel C 1988 *Phys. Rev.* A **38** 6296
[4] van den Berg H P and Hoheisel C 1990 *Phys. Rev.* A **42** 2090
[5] Trullas J and Padro J A 1993 *J. Chem. Phys.* **99** 3983
     Trullas J and Padro J A 1994 *Phys. Rev.* E **50** 1162
[6] Raineri F O and Friedman H L 1989 *J. Chem. Phys.* **91** 5633
     Raineri F O and Friedman H L 1989 *J. Chem. Phys.* **91** 5642
[7] Allen M P and Tildesley D J 1986 *Computer Simulation of Liquids* (Oxford: Clarendon)
[8] Gonzalez L E, Gonzalez D J, Meyer A and Silbert M 1996 *J. Phys.: Condens. Matter* **8** 4465
[9] Lee J C 1997 *Physica* A **243** 229
[10] Zhou Y and Miller G H 1996 *Phys. Rev.* E **53** 1587
[11] Denton A R and Egelstaff P A 1997 *Z. Phys.* B **103** 343
     Salacuse J J, Denton A R and Egelstaff P A 1996 *Phys. Rev.* E **53** 2382
[12] Mori H, Hoshino K and Watabe W 1991 *J. Phys.: Condens. Matter* **3** 9791
[13] Hansen J-P and McDonald I R 1986 *Theory of Simple Liquids* 2nd edn (London: Academic)
[14] Baumketner A and Chushak Ya 1999 *J. Non-Cryst. Solids* at press
[15] Galam S and Hansen J-P 1976 *Phys. Rev.* A **14** 816
[16] Kambayashi S and Chihara J 1994 *Phys. Rev.* E **50** 1317
[17] Hultgren R R, Orr R L, Anderson P D and Kelly K K 1963 *Selected Values of Thermodynamic Properties of Metals and Alloys* (New York: Wiley)
[18] Alblas B P and van der Lugt W 1980 *J. Phys. F: Met. Phys.* **10** 531
[19] Boon J P and Yip S 1980 *Molecular Hydrodynamics* (New York: McGraw-Hill)
[20] Gudowski W, Dzugutov M and Larsson K-E 1993 *Physica* A **201** 441